A general model for allometric covariation in botanical form and function

Charles A. Price*†, Brian J. Enquist*‡, and Van M. Savage§

*Department of Ecology and Evolutionary Biology, University of Arizona, Tucson, AZ 85721; ‡Sante Fe Institute, 1399 Hyde Park Road, Santa Fe, NM 87501; and §Department of Systems Biology, Harvard Medical School, Boston, MA 02115

Edited by Karl J. Niklas, Cornell University, Ithaca, NY, and accepted by the Editorial Board June 14, 2007 (received for review March 11, 2007)

The West, Brown, and Enquist (WBE) theory for the origin of allometric scaling laws is centered on the idea that the geometry of the vascular network governs how a suite of organismal traits covary with each other and, ultimately, how they scale with organism size. This core assumption has been combined with other secondary assumptions based on physiological constraints, such as minimizing the scaling of transport and biomechanical costs while maximally filling a volume. Together, these assumptions give predictions for specific ''quarter-power'' scaling exponents in biology. Here we provide a strong test of the core assumption of WBE by examining how well it holds when the secondary assumptions have been relaxed. Our relaxed version of WBE predicts that allometric exponents are highly constrained and covary according to specific quantitative functions. To test this core prediction, we assembled several botanical data sets with measures of the allometry of morphological traits. A wide variety of plant taxa appear to obey the predictions of the model. Our results (*i*) underscore the importance of network geometry in governing the variability and central tendency of biological exponents, (*ii*) support the hypothesis that selection has primarily acted to minimize the scaling of hydrodynamic resistance, and (*iii*) suggest that additional selection pressures for alternative branching geometries govern much of the observed covariation in biological scaling exponents. Understanding how selection shapes hierarchical branching networks provides a general framework for understanding the origin and covariation of many allometric traits within a complex integrated phenotype.

allometry | fractal | metabolism | scaling | traits

Since the pioneering work of Julian Huxley (1), questions concerning how selection influences specific traits within integrated phenotypes have been a prominent focus in comparative biology (2, 3). The phenotype is a constellation of traits that often covary with each other during ontogeny. Further, organism size is a central trait that influences how most biological structures, processes, and dynamics covary with each other (4, 5). The dependence of a given biological trait, Y, on organismal mass, M, is known as allometry. Allometric relationships are often characterized by power laws (1) of the form, $Y = Y_0 M^{\theta}$, where θ is the scaling exponent and Y_0 is a normalization constant that may be characteristic of a given taxon. A sampling of intra- and interspecific data reveals that the central tendency of θ often approximates quarter-powers (4, 5) (e.g., 1/4, 3/4, 3/8, etc.), although for any given relationship considerable variability may exist (6).

West, Brown, and Enquist (7–9) hypothesized that the value of θ for many biological allometries arises from the geometry of vascular networks and resource-exchange surfaces (e.g., cardiovascular or plant vascular systems). The core assumption of this theory is that many organismal, anatomical, and physiological traits are linked mechanistically by allometric scaling of the vascular network. For example, for plants, whole-plant carbon assimilation or gross photosynthesis, P, vascular fluid flow rate, Q_0, and the number, n_L, and mass, M_L, of leaves are all assumed to vary or scale proportionally with one another, and ultimately with plant mass (M), to the power θ as $P \propto Q_0 \propto n_L \propto M_L \propto M^{\theta}$. In addition, several other hydrodynamic and anatomical attributes of plant hydraulics and branching morphology are also determined by θ (7, 8, 10–14): specifically, the value of $\theta = 1/(2a + b)$, where a and b characterize the geometry of the vascular network within a given species. Within the model, network geometry and gross morphology are characterized by three parameters:

$$\gamma_k \equiv \frac{l_{k+1}}{l_k} \equiv n^{-b} \quad \beta_k \equiv \frac{r_{k+1}}{r_k} \equiv n^{-a} \quad \bar{\beta}_k \equiv \frac{r_{T,k+1}}{r_{T,k}} \equiv n^{-\bar{a}/2}, \qquad [1a–c]$$

which respectively refer to the ratios of branch lengths, external branch radii, and internal tube radii (e.g., xylem vessels or tracheary elements) between k adjacent branching levels (Fig. 1). The value of n is the furcation ratio or number of daughter branches per parent branch. Note that we differ in notation from the original model (8) that defined the branch radii ratio as $n^{-a/2}$, the internal tube radii as $\bar{a}$, and the lengths ratio as $n^{-1/3}$. Importantly, here we allow the length and the radii ratios to be continuous traits defined by arbitrary powers b and a, respectively.

The origin of quarter-power scaling emerges when a and b take specific values, $a = 1/2$ and $b = 1/3$, thus yielding $\theta = 3/4$. This $\theta = 3/4$ rule emerges from four assumptions: (*i*) that the network is volume-filling; (*ii*) that the minimum total work to move fluid through the network corresponds to minimizing the hydrodynamic resistance in a single tube; (*iii*) that properties of an individual leaf (e.g., M_L, P_L, Q_L) are independent of plant size; and (*iv*) that biomechanical constraints are uniform (8). Extensions of The West, Brown, and Enquist (WBE) theory for the origin of allometric scaling laws model have shown how factors secondary to organism size, such as temperature and stoichiometry (15), can influence residual variation or the normalization (Y_0) of allometric scaling relationships.

Recently, several prominent critics (6, 16) have argued that the WBE model cannot explicitly account for the range and origin of inter- and intraspecific variability in allometric exponents. Further, the assumption of the primacy of the vascular network, although implicit in the original work, has not been explicitly tested (17). Indeed, although detailed treatments of WBE have been applied to the origin of the $\theta = 3/4$ rule in the vascular networks of animals (7) and plants, including stem branching (8, 12) and leaf venous (13) networks, it is not clear whether the WBE model can account for all, or even most, of the observed variation in allometric exponents or for how traits covary allometrically within integrated phenotypes.

Author contributions: C.A.P. and B.J.E. designed research; C.A.P. and V.M.S. performed research; C.A.P., B.J.E., and V.M.S. analyzed data; and C.A.P., B.J.E., and V.M.S. wrote the paper.

The authors declare no conflict of interest.

This article is a PNAS Direct Submission. K.J.N. is a guest editor invited by the Editorial Board.

Abbreviation: WBE, West, Brown, and Enquist theory.

†To whom correspondence should be sent at the present address: Department of Biology, Georgia Institute of Technology, Atlanta, GA 85721. E-mail: cprice6@mail.gatech.edu.

This article contains supporting information online at www.pnas.org/cgi/content/full/0702242104/DC1.

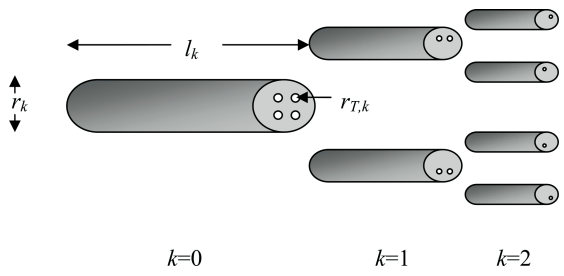

Fig. 1. An idealized hierarchical branching network from level 0 to level *N*. Each branching generation can be described by its length (l_k), its branch radius (r_k), and its internal tube radius ($r_{T,k}$). Here there are two generations beyond the initial branch, so $N = 2$, and there are two daughter branches per parent branch, so $n = 2$. At any level k, there are n^k branches. For example, when $k = 2$, $n^k = 2^2 = 4$.

Here we address these questions and criticisms by presenting a unique extension of the WBE theory. Specifically, we show how continuous variation in the fractal exponents allows us to assess whether the observed variation in allometric exponents is due to violations of the secondary assumptions that lead to quarter-power scaling and, if so, whether the variation is consistent with covariation in allometric traits as governed by vascular network geometry.

Model Extension

We start with the observation that many plants do not conform to the optimizing assumptions in the original WBE derivation (8, 12, 18). For example, succulents, palms, saplings, ground-spreading forbs, vines, lianas, and herbaceous plants with photosynthetic stems all have morphologies that strictly violate one or more of the assumptions of the original model (13). However, according to the framework of the WBE model, such plants with divergent morphologies may be characterized by differing values of a and b. Here we investigate whether such variation in branching geometry can lead to predictable covariation in allometric traits, as dictated by the core assumption of the WBE model. We also ask whether such diverse, allometrically integrated phenotypes can be attributed to selection for unique morphologies and life histories. If this approach holds, then our relaxed version of the WBE model predicts that plants that violate the secondary assumptions, and hence differ from canonical quarter-power relationships, will be characterized by allometric scaling exponents that follow specific covariation functions.

To examine the departure from space-filling and energy-minimizing branching, we highlight six allometric scaling relationships in terms of the scaling of photosynthetic surface area (A_S), stem radius (r_0), height (l), and whole-plant mass (M) [see supporting information (SI) *Methods* for the complete model derivation]. Each relationship can be expressed in terms of continuous traits dependent on network geometry (as defined in Eq. **1 a** and **b**), where

$$A_S \propto M^{\theta} \quad r_0 \propto M^{a\theta} \quad l_0 \propto M^{b\theta} \qquad \textbf{[2a–c]}$$

and

$$l_0 \propto r_0^{b/a} \quad A_S \propto r_0^{1/a} \quad A_S \propto l_0^{1/b}. \qquad \textbf{[3a–c]}$$

According to the central assumption of the WBE model, covariation between each of these traits (A_S, l_0, r_0, and M) is governed by the geometry (i.e., the values of a and b) of the branching network. As a result, departures from the secondary assumptions of volume-filling and area-preserving in the original WBE derivation (where $b = 1/3$, $a = 1/2$) will yield different values of b and a, and hence, θ.

According to Eqs. **2** and **3**, an expanded version of the WBE model that emphasizes the continuous nature of branching geometry predicts that observed variation in allometric exponents is due to variation in the fractal network exponents a and b. In some environments, natural selection has likely acted to optimize network geometry in ways that violate the original secondary assumptions. If such variability in selection has resulted in diverse network designs, then we expect that a and b will also vary. As a result, our model shows that variation in the scaling of botanical form and function, as reflected by Eqs. **1–3**, is described by a highly constrained continuum of unique allometric scaling exponents (Table 1). For example, our model predicts that across species, a plot of the intraspecific exponent from the relationship between stem radius and mass (i.e., $a\theta$ from $r_0 \propto M^{a\theta}$) vs. the intraspecific allometric relationship from the relationship between branch length and radius (i.e., b/a from $l_0 \propto r_0^{b/a}$) will be described by the covariation curve $a\theta = 1/[2 + (b/a)]$. Similarly, additional covariation functions can be derived to quantify the scaling of additional phenotypic traits (e.g., r_0, l_0, A_S, and M) (see Table 1 and *SI Methods*). We note that it is also possible to derive additional predictions for continuous allometric covariation for several other hydraulic, anatomical, and physiological traits, as listed by West *et al.* (7, 8).

Table 1. Plots and covariation curves for the relationships presented in Figs. 2 and 3

Plot	Covariation curve
Fig. 2*a* ($a\theta$ vs. b/a)	$a\theta = 1/[2 + (b/a)]$
Fig. 2*b* ($b\theta$ vs. b/a)	$b\theta = 1/[1 + 2/(b/a)]$
Fig. 2*c* ($a\theta$ vs. $b\theta$)	$a\theta = (1 - b\theta)/2$
Fig. 3 [b (z axis) vs. $b\theta$ (y axis) vs. θ (x axis)]	$b\theta = b^*\theta$ (i.e., $y = zx$)
Fig. 3 (dashed line, where $a = 1/2$)	$b\theta = b/(b + 1)$
Fig. 3 (dashed-dotted line, where $b = 1/3$)	$b\theta = 1/(6a + 1)$

Each function is determined entirely by the biologically meaningful parameters a and b, and thus there are no free parameters in these covariation functions.

To test the predictions outlined by Eqs. **2** and **3** and Table 1, we used data from our own compilation and from several published studies, limiting analyses to studies that measured more than one intraspecific allometric scaling exponent (see SI Tables 2 and 3 and Figs. 2 and 3). Fig. 2 shows each of the predicted covariation functions (Table 1). Our relaxed version of the WBE model provides a good description of allometric covariation in real plants, inasmuch as the empirical data closely follow the predicted lines (see *Methods* for statistics).

Figs. 2 and 3 lead to an important question: What ultimately governs the observed variation in the parameters a and b and, thus, in the fractal relationships for the branch radii and lengths? Understanding such variation will likely provide insight into how selection determines plant form, function, and diversity by means of vascular network geometry. We give two mechanistic examples of how selection for specific functional properties, as realized by branching morphologies, has likely resulted in the observed range in allometric covariation in the traits shown in Figs. 2 and 3.

Selection to Minimize Total Plant Hydraulic Resistance and Path Length. Within species or functional groups for which vascular conductance is not limiting to plant metabolism or carbon balance, the assumption that the total hydraulic resistance is always minimized may not be strictly upheld; this would then lead to differential variation in a and b. Within the WBE model, hydraulic resistance (Z) to flow in xylem elements is described by the Poiseuille equation, $Z = 8\mu l/\pi r_T^4$ (8). Assuming that viscosity, μ, is constant, resistance will increase linearly with length, l, but inversely with the fourth power of the tube radius, r_T. Additionally, if interspecific variation in internal tube radii (r_T) is more closely tied to variation in external branch radii than it is to interspecific height (or branch length), then variation in plant stem radius and height will both correspond to variation in whole-plant hydraulics (8). If these

PLANT BIOLOGY

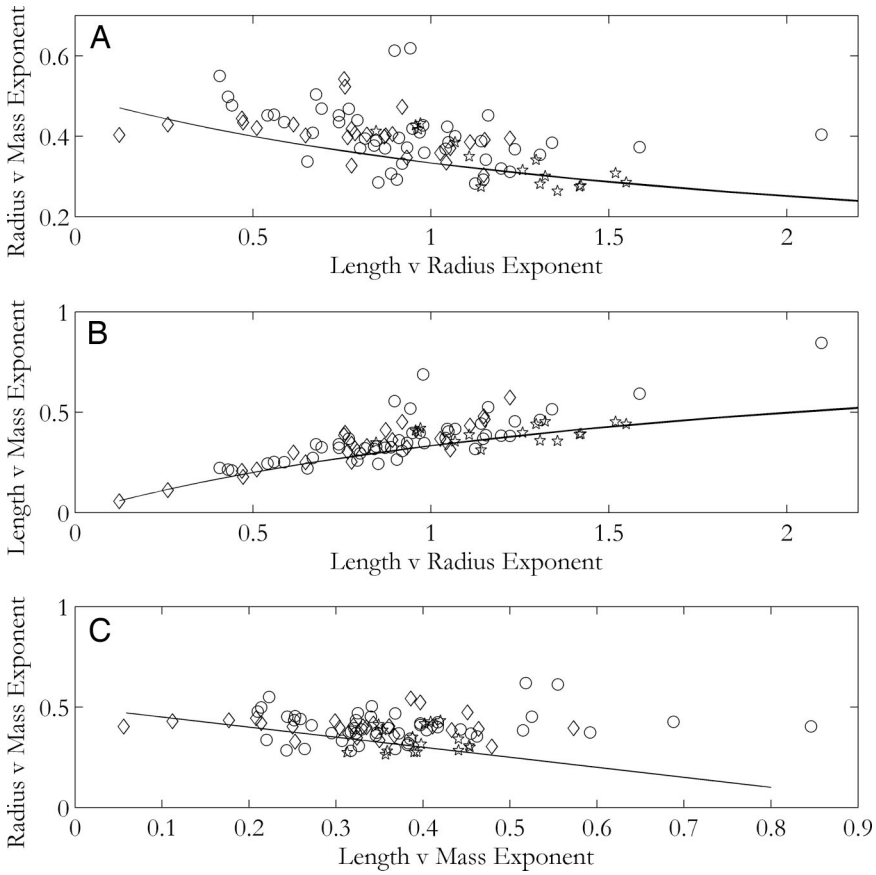

Fig. 2. Allometric covariation of whole-plant morphology and mass. The axes represent the exponents for the scaling relationships described by Eqs. **2b** (*A*), **2c** (*B*), and **3a** (*C*) (Table 1). Symbols represent observed exponent values for Sonoran Desert plant species (circles), trees from the Cannell forestry database (diamonds), and angiosperm leaves (pentagrams). Black lines bisecting the data represent predicted covariation functions (Table 1), letting b and a vary from 1 to 1/8. Note that when $n = 2$, a or $b = 1/8$ corresponds to a lengths or radii ratio of 0.92 or, for example, a daughter branch that is 92% as long as its parent branch. The predicted line is completely determined, contains no free parameters, and spans at least 89% of the values on the abscissa when b and a vary from 1 to 1/3. The data are from 27 families representing herbaceous annuals and perennials, succulents, and both angiosperm and gymnosperm trees and thus constitute a broad sampling of tracheophytes. Related data are presented in SI Tables 2 and 3.

assumptions are approximately correct, then selection on variation in the scaling of whole-plant branch lengths (reflected in b) will have much less impact on the total resistance than selection on variation in the scaling of branch radii (reflected in a). Thus, the principal axis of morphological variation in plants will be described by changes in the ratio of branch lengths, or γ (or b), whereas changes in radii, or β (or a), will be a smaller secondary axis. This asymmetry in b and a is consistent with our empirical observations of allometric covariation. In agreement with our prediction, Fig. 3 displays substantially larger variation in empirical exponents along the axis described by variability in lengths ratios, b. Additional hydrodynamic variability may result from variation in network tapering ($\bar{a}$) and/or total path length (L_T) (see *Methods*).

The degree of volume-filling branching likely reflects costs associated with the collection of resources because branching architecture is closely linked with light-gathering in leaves and limbs and with water/nutrient-gathering in roots (19). Because the equation for volume filling, $l_k^3 = nl_{k+1}^3$ (Eq. **1a**) increases with the cube of branch lengths, l^3 (7, 8), but does not depend on branch radii, any selection on variation in volume-filling must necessarily strongly constrain variation in the scaling of branch lengths (i.e., b) but not branch radii (i.e., a).

Three possible scenarios have likely controlled the observed variation in the scaling of botanical lengths and radii. (*i*) If selection has acted to primarily minimize hydrodynamic resistance, then variation in the fractal exponents for lengths, b, will be considerably greater than for radii, a. (*ii*) On the other hand, if selection has primarily acted to maximize the volume-filling nature of the branching network, then variation in the observed fractal exponents for radii, a, will be unbounded and thus considerably greater than variation in length exponents, b, which will be tightly constrained. (*iii*) If, however, selection has simultaneously minimized the hydrodynamic resistance (which depends on r_T^4) and maximized the volume-filling nature of the branching (which depends on l^3), then the observed variation in fractal exponents for stem radii, a, will be slightly greater than the variation in exponents for lengths, b. Our data support the first scenario. Observed covariation in botanical allometric data are consistent with greater variation in lengths than variation in radii (Fig. 3). If our reasoning is correct, then the observed covariation in allometric traits across extant phenotypes is consistent with the expectation that selection to maximize the volume-filling nature of the branching network has not been as strong as selection to minimize the hydrodynamic resistance of the network.

Variability in Biomechanical Constraints. Additional variability in plant scaling exponents likely also reflects violations of the biomechanical constraints originally assumed by the WBE model, e.g., biomechanical demands that change systematically with size and, in particular, with stem diameter (20–23). To resist elastic buckling due to self-loading, plants must invest in higher density structural tissue, lignin, cellulose, etc., to resist increasing tensive and com-

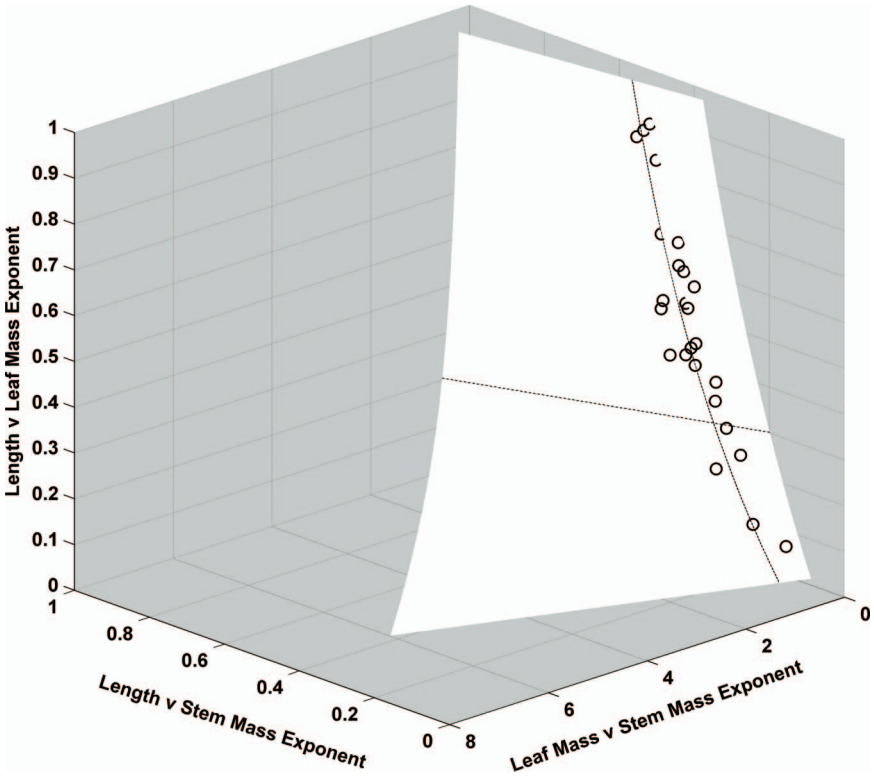

Fig. 3. Allometric covariation of whole-plant morphology and biomass partitioning. Open circles represent empirical intraspecific exponents from the Cannell forestry database (52) (see SI Table 3). The white surface represents predicted combinations of exponents (Table 1). The vertical dashed line represents the predicted covariation function (given in Table 1) holding *a* constant at ½ and letting *b* vary from 1 to 1/20 (1/20 corresponds to a lengths ratio of 0.97 when $n = 2$). The horizontal dashed-dotted line represents the same equation (Table 1) but instead holding *b* constant at 1/3 and letting *a* vary again from 1 to 1/20. The intersection of these two functions represents the predictions from the original WBE model. As predicted, the major axis of variation is consistent with changes in branch lengths (*b*), whereas the secondary axis is consistent with changes in radii (*a*), which are hypothesized to be more tightly constrained. Note that 19/25 (76%) data points are contained within the surface described by letting *a* and *b* both vary from 1 to 1/3. Those that fall outside of this range may result from violations of the model's assumptions discussed in the text, such as departures from self-similarity.

pressive forces. The theoretical height to which a beam can be extended before it buckles under its own weight (l_{crit}) was considered by Greenhill (22) and was represented as a function of the radius and density-specific stiffness of the beam. Thus, Eq. **3a** can be expressed as

$$l_{crit} \propto r^{\frac{b}{a}} \propto C\left(\frac{E}{\rho}\right)^{1/3} r^{2/3}, \qquad [4]$$

where E is Young's elastic modulus, ρ is bulk tissue density (kilograms per cubic meter), and C is a proportionality constant. Previous solutions to the bending moment equation that have given $b/a = 2/3$ have assumed that density-specific stiffness (E/ρ) is a constant (8). However, as has been noted by Niklas (21, 24), if E/ρ varies systematically within or across plants, then the scaling of height with radius will vary (25). Specifically, if E/ρ increases with stem radius, then $b/a > 2/3$, and if E/ρ decreases with stem radius $b/a < 2/3$. Limited data from a literature search suggest that the density-specific strength of plant tissues increases as one goes from herbaceous to woody taxa (see SI Fig. 4), so E/ρ is unlikely to be constant, and the interspecific scaling of height with diameter is likely to have a slope >2/3 when herbaceous taxa are included in the analysis. Our compiled data strongly support this hypothesis (see SI Fig. 5).

Discussion

Understanding the physiological constraints governing the scaling of organic form has intrigued biologists since Aristotle and Galileo and has spawned several classic synthetic works (1, 4, 26, 27). A number of models have been proposed to explain the mechanistic basis for the diversity of organic form and function. These models include geometric similarity (28), elastic and stress similarity (20), and more recent work invoking energy minimization in hierarchical volume-filling networks (7, 8). These models are similar in predicting unique exponents for a particular scaling relationship (e.g., $l_0 \propto r_0^{2/3}$ or $B \propto M^{3/4}$). Tests of the predictions of these models typically involve fitting regression lines to empirical data, followed by a discussion regarding whether the confidence intervals for an observed fitted exponent include or exclude a certain model. However, this approach often leads to vigorous debate as to which model better fits the data. A recent example of this is the protracted discussion as to whether the scaling of whole-organism metabolic rate with body mass is better fit with a slope of 2/3 or 3/4 (29, 30).

Our approach is a natural extension of previous work (7, 8) because it explicitly addresses variation in network design. However, our extended version of the WBE model is unique in that it recognizes the primary importance of vascular networks while simultaneously emphasizing the continuous nature of allometric phenomena in biology within all organisms that contain hierarchical vascular networks. In so doing, we explicitly acknowledge that no specific network geometry will describe all organisms. For example, arguments based on heat dissipation in geometrically similar organisms (28), elastically similar branching networks (20), or energy minimization in fractal distribution networks (7, 8) all fall along the continuum of variation we have predicted. Importantly, the optimization argument of the WBE model does predict a zeroth-order approximation, or basin of attraction, around which actual biological networks cluster and provides a baseline for

identifying these deviations. It is likely that departures from these classic results represent an organism's attempt to optimize the constraints listed above while meeting additional ecological challenges. For example, when looking within functional group categories, the central tendency within allometric exponents for herbaceous annual plants differs from that of woody species (see SI Table 4). In contrast, the central tendency within woody species from different data sets is quite similar.

Although variation in allometric exponents has long been observed (4, 27), there is currently no generally agreed-on theory for understanding just how this variation is related to allometrically integrated phenotypes (31). Our model begins to address this void. We hypothesize that the fundamental source of variation in allometric relationships is variation in network geometry. Our relaxed version of the WBE model quantitatively predicts mathematical functions that describe continuous covariation in the scaling of many phenotypic traits. Consequently, our model provides a more quantitative and integrative characterization of allometric data.

Because of the intense interest and controversy surrounding the WBE model and its descendents, a brief digression regarding the philosophy of our approach is perhaps warranted. To quote the noted 20th century statistician George Box (32), "All models are wrong, some models are useful." We fully acknowledge that the model presented herein is but an abstraction of a very detailed and complicated botanical world. Our hope is to describe as much of that variability with as few, biologically meaningful, parameters as possible. In this respect, we feel that our model is indeed quite useful.

This article is an attempt to examine, both theoretically and empirically, the allometric covariation of traits across a broad array of plant functional types. Moreover, our model agrees quite well with the data. A conservative interpretation of this agreement is that some covariation is inevitable, based simply on changes in shape alone. A more liberal interpretation is that the geometry of biological networks does indeed correspond strongly with plant gross morphology and can be used to predict and interpret allometric variability. Indeed, that correlations between allometric exponents increase or decrease together is somewhat intuitive. However, the exact quantitative covariation curves that our model describes are not intuitive and follow directly from details of the branch and vascular networks. We are unaware of alternative models that predict covariation among allometric exponents on the basis of changes in shape, network geometry, or otherwise.

Our model further provides a basis for understanding how additional selection on differing aspects of network geometry will influence covariation in allometric traits. A key result of this approach is that it provides insight into the important selective forces that have likely guided the diversification of plant morphology and network architecture, and hence allometric exponents (i.e., more variation in the scaling of lengths than diameters). In addition to the factors mentioned previously, features such as departures from self-similarity, variation in hydraulic diameter (33), disconnect between internal and external branching (18), or volume loss across branching generations likely explain much of the variation not accounted for by our work here. These important aspects of biology can be incorporated into more detailed efforts in the future. For example, as shown by Turcotte *et al.* (34), networks that do not have strictly self-similar branching, such as those with side branches, can still be described by exponents generated from models that assume a self-similarity, provided the side branches bear the correct relationship to the mean branching properties.

We recognize that our approach is predicated on a couple of important assumptions, specifically, (*i*) that real biological networks are themselves statistically self-similar or "fractal-like" (7) and (*ii*) that the range of values for a and b matches that for the gross morphology of plants. Many vascular networks appear superficially fractal-like; however, detailed studies quantitatively characterizing vascular network geometry (i.e., measuring the branch lengths and radii ratios described in Eq. **1 a–c**), are quite rare. Although fractal-like morphologies have been reported in a variety of taxa (35), it is likely that numerous examples exist of biological networks (internal or external) that depart in very real and meaningful ways from self-similarity. It is encouraging that the limited number of studies reporting data for branch length or radii ratios have reported values consistent with the range we invoke here (34–42).

WBE has been criticized for its inability to account for much of the variation in real organisms, particularly with respect to the scaling of metabolic rate (16, 43, 44). Our work addresses these concerns by demonstrating that the scaling of metabolic rate in all organisms is likely determined primarily by the dimension of the volume that the organism fills ($1/b$), the length of the network within the organism (L_T), and the extent to which area-preserving ($a = 1/2$) or area-increasing ($a < 1/2$) branching dominates. For example, in small volume-filling organisms in which the distribution networks have only a few branching generations, flow rates must slow to allow for nutrient diffusion across vessel walls, and thus area-increasing branching ($a \approx 1/3$) may dominate, suggesting that θ should approach 1 (14, 44). A similar approach can be used to describe scaling in very small plants and leaves that behave more like plane-filling networks ($b \rightarrow 1/2$) with area-increasing branching ($a \approx 1/3$) (13, 43). It should be noted that the range of biologically likely values, $b \rightarrow 1$ and $a = 2$, as well as $b = 3$ and $a = 3$, yield $B \propto M^{1/2}$ and $B \propto M^1$, respectively. These values bound the most commonly reported exponents and provide a context within which to interpret the variation we observe in the empirical data.

We have shown here that covariation in morphological allometry and biomass partitioning is consistent with the primacy of network geometry. However, allometric covariation can best be understood by considering a continuum of branching geometries, comparing this continuum to data, and investigating departures from the strict WBE model, and in particular, which biologically motivated assumptions need to be relaxed. Such an approach offers insight into additional, selective pressures that have likely shaped the evolution of the diversity of plant form and function. More importantly, our results indicate that a common body of allometric theory potentially provides a framework for understanding the mechanistic origin of trait covariation within complex phenotypes.

Methods

To test the predictions of our model, we determined the intraspecific exponents for the relationships described above (Eqs. **2** and **3**) and plotted these exponents against one another. The data in Figs. 2 and 3 correspond to the data in SI Tables 2 and 3, respectively. For each bivariate relationship, we also overlaid a predicted covariation function (Table 1) and allowed the theoretical exponents to vary over a biologically meaningful range (see Figs. 2 and 3 legends). Five of the six bivariate relationships examined had standardized major axis regression slopes significantly different from zero ($P \ll 0.05$), with the exception being the relationship depicted in Fig. 2*c*.

We evaluated support for our model in three ways. First, we used the fact that for the three relationships presented in Fig. 2, the exponent on each y axis can be predicted as a function of the exponent on the x axis. These functions are described in the first three rows of Table 1. For example, substituting our empirical exponents for the l_0 vs. r_0 relationship (b/a) into $a\theta = 1/[2 + (b/a)]$ predicts a line of unity (1:1). Using this method and fitting ordinary least-squares regression (OLS) slopes to each of these three relationships yields lines not statistically different from unity in two of the three cases [note that OLS regression is recommended when predicting Y from X (45, 46)]. Using the l_0 vs. r_0 exponent (b/a) to predict the r_0 vs. M ($a\theta$) exponent yields a slope of ≈1.00 and 95% confidence intervals (0.65–1.36) that include 1 ($R^2 = 0.27$). Similarly, using the l_0 vs. r_0 exponent (b/a) to predict the l_0 vs. M ($b\theta$) exponent gives a slope of ≈1.21 and 95% confidence intervals (1.00–1.41) that again include 1 ($R^2 = 0.61$). Using the observed l_0

vs. M exponent to predict the r_0 vs. M exponent yields a slope not different from zero ($P = 0.96$).

Second, because the above method cannot be extended to the bivariate relationships in Fig. 3 given that the predicted function is a manifold, and not a line, we used an alternative approach. For the three relationships shown in Fig. 3, we simply counted the number of data points that fell within the hypothesized bounds (letting a and b vary from 1 to 1/3). A total of 19/25 points (76%) fell within our hypothesized bounds in each relationship. Points that fall outside of this range may result from violations of the model's assumptions discussed in the text, such as departures from self-similarity.

Third, to test whether the density-specific stiffness of plant tissue varied systematically with plant size, we collected data for both herbaceous (47) and woody (19, 48, 49) taxa from the primary literature. Standardized major axis regression of log-transformed density-specific stiffness against basal stem diameter yields positive slopes for both functional groups (see SI Fig. 4) (45).

Data to test the predictions of our model came from two sources. In gathering our data, we only used cases in which all three exponents in Figs. 2 and 3 had been measured independently. First, one of us (C.A.P.) measured height (millimeters, l_0), basal stem diameter (millimeters, r_0), and dry mass (grams, M) in 1,264 individual plants (44 species, mean $\approx$ 28.7 plants per species) spanning >8 orders of magnitude in above-ground dry mass and including herbaceous annuals and perennials, succulents and woody species. To our knowledge, this is the largest existing allometric database on arid-land plants. Further, a total of 464 angiosperm leaves in 16 species were collected, with $\approx$30 leaves per species (see SI Table 2). Leaf length (millimeters, l_0), stem diameter (millimeters, r_0), and leaf dry mass (grams, M) were measured, and these data span the range of sizes available for each species. Leaf data were included in the analyses for two primary reasons: (*i*) many herbaceous species are composed of little more than leaves, thus data for the scaling of leaf dimensions likely closely approximate scaling for many small herbaceous taxa, and (*ii*) leaves themselves are filled with vascular distribution networks and are subject to many, if not all, of the same selective pressures facing whole plants, thus the scaling arguments presented herein can also be applied to leaves (13).

Second, data on the scaling of plant total leaf mass (M_L), plant stem mass (M_S), radius (r_0), and height (l_0) (Figs. 2 and 3 and SI Tables 2 and 3) are from the Cannell data compendium (50), which reports mean biometric values for even-aged stands. Note that the model predicts isometry between the scaling of total leaf mass (M_L) and total leaf area ($M_L \propto A_S^1$) and also isometry between the scaling of plant stem mass (M_S) and whole-plant mass ($M_S \propto M^1$) (51). Thus, we substitute M_L for A_S in Eqs. **2a** and **3c** and similarly substitute M_S for M in Eq. **2 a** and **c**. We looked at allometric relationships among the three previously mentioned variables for those species represented by at least eight stands.

In the interest of minimizing the impact on native plant communities, all Sonoran Desert plants were collected from three construction sites, where they were slated for destruction, in the greater Tucson, AZ, region during the 2001 and 2002 summer field seasons. Site 1 was along a road-widening easement (lat/long: 32°318′N, 111°011′W; elevation: ≈705 m) in North Tucson. Site 2 was a resort golf course installation (lat/long: 32°206′N, 111°052′W; elevation: ≈795 m) in West Tucson. Site 3 was within the Desert Laboratory at Tumamoc Hill in Central/West Tucson (lat/long: 32°210′N, 11°042′W; elevation: ≈710 m). Measurements (save mass) for all plants were taken in the field before collection.

V.M.S. gratefully acknowledges Walter Fontana and his laboratory for support and enlightening conversations. C.A.P. and V.M.S. wish to acknowledge the Australian Research Council–Landcare Research New Zealand (ARC-NZ) Research Network for Vegetation Function for the opportunity to participate in a stimulating working group on this subject. We thank David Ackerly, Joshua Weitz, and an anonymous reviewer for helpful comments on earlier drafts of this manuscript. C.A.P. was supported by the Ecological Society of America's Forrest Shreve Award, The William G. McGinnies Scholarship in Arid Land Studies at the University of Arizona, and National Science Foundation (NSF) funding (to B.J.E.). B.J.E was supported by an NSF CAREER Award, a Los Alamos National Laboratories grant, and a Fellowship from Conservation International.

1. Huxley JS (1932) *Problems of Relative Growth* (Methuen, London).
2. Coleman J, McConnaughay K, Ackerly D (1994) *Trends Ecol Evol* 9:187–191.
3. Murren C (2002) *Plant Species Biol* 17:89–99.
4. Calder WA, III (1984) *Size, Function, and Life History* (Harvard Univ Press, Cambridge, MA).
5. Schmidt-Nielsen K (1984) *Scaling: Why Is Animal Size So Important?* (Cambridge Univ Press, Cambridge, UK).
6. Glazier DS (2005) *Biol Rev* 80:611–662.
7. West GB, Brown JH, Enquist BJ (1997) *Science* 276:122–126.
8. West GB, Brown JH, Enquist BJ (1999) *Nature* 400:664–667.
9. West GB, Brown JH, Enquist BJ (1999) *Science* 284:1677–1679.
10. West GB, Brown JH, Enquist BJ (2000) in *Scaling in Biology*, eds Brown JH, West GB (Oxford Univ Press, Oxford, UK), pp 87–112.
11. Enquist BJ, West GB, Brown JH (2000) in *Scaling in Biology*, eds Brown JH, West GB (Oxford Univ Press, Oxford, UK), pp 167–199.
12. Enquist BJ (2002) *Tree Physiol* 22:1045–1064.
13. Price CA, Enquist BJ (2007) *Ecology* 88:1132–1141.
14. Enquist BJ, Allen AP, Brown JH, Kerkhoff AJ, Niklas KJ, Price CA, West GB (2007) *Nature* 445:E9–E10.
15. Kerkhoff AJ, Enquist BJ, Elser JJ, Fagan WF (2005) *Global Ecol Biogeogr* 14:585–598.
16. Bokma F (2004) *Funct Ecol* 18:184–187.
17. Ricklefs R (2003) *Funct Ecol* 17:384–393.
18. Price CA, Enquist BJ (2006) *Funct Ecol* 20:11–20.
19. Küppers M (1989) *Trends Ecol Evol* 4:375–379.
20. McMahon TA, Kronauer RE (1976) *J Theor Biol* 59:443–466.
21. Niklas KJ (1994) *Plant Allometry: The Scaling of Form and Process* (Univ Chicago Press, Chicago).
22. Greenhill AG (1881) *Proc Cambridge Phil Soc* 4:65–73.
23. Niklas KJ (1997) *Ann Bot (London)* 79:265–272.
24. Niklas KJ (1997) *Ann Bot (London)* 79:479–485.
25. Niklas KJ, Spatz H-C (2004) *Proc Natl Acad Sci USA* 101:15661–15663.
26. Thompson DAW (1942) *On Growth and Form* (Cambridge Univ Press, Cambridge, UK).
27. Peters RH (1983) *The Ecological Implications of Body Size* (Cambridge Univ Press, Cambridge, UK).
28. Rubner M (1883) *Z Biol* 19:535–562.
29. Heusner AA (1982) *Respir Physiol* 48:1–12.
30. Savage VM, Gillooly JF, Woodruff WH, West GB, Allen AP, Enquist BJ, Brown JH (2004) *Funct Ecol* 18:257–282.
31. Farnsworth KD, Niklas KJ (1995) *Funct Ecol* 9:355–363.
32. Box GEP (1979) in *Robustness in Statistics*, eds Launer RL, Wilkinson GN (Academic, New York), pp 1–17.
33. Lewis AM (1992) *Am J Bot* 79:1158–1161.
34. Turcotte DL, Pelletier JD, Newman WI (1998) *J Theor Biol* 193:577–592.
35. Abraham ER (2001) *Mar Biol* 138:503–510.
36. Canny MJ (1990) *New Phytol* 114:341–468.
37. McCulloh KA, Sperry JS, Adler FR (2003) *Nature* 421:939–942.
38. LaBarbera M (1990) *Science* 249:992–1000.
39. Krogh A (1920) *Pflügers Arch Gesamte Physiol Menschen Tiere* 179:95–112.
40. Horn HS (2000) in *Scaling in Biology*, eds Brown JH, West GB (Oxford Univ Press, Oxford), pp 199–220.
41. Shinozaki K, Yoda K, Hozumi K, Kira T (1964) *Jpn J Ecol* 14:133–139.
42. Huber B (1928) *Jahrb Wiss Bot* 67:877–959.
43. Reich PB, Tjoelker MG, Machado J-L, Oleksyn J (2006) *Nature* 439:457–461.
44. Glazier DS (2006) *Bioscience* 56:325–332.
45. Warton DI, Wright IJ, Falster DS, Westoby M (2006) *Biol Rev* 81:259–291.
46. Sokal RR, Rohlf FJ (1995) *Biometry* (Freeman, New York).
47. Niklas KJ (1995) *Ann Bot (London)* 75:217–227.
48. Alden HA (1995) *Hardwoods of North America* (US Department of Agriculture, Forest Service, Forest Products Laboratory, Madison, WI), Gen Tech Rept FPL-GTR-83.
49. Alden HA (1997) *Softwoods of North America* (US Department of Agriculture, Forest Service, Forest Products Laboratory, Madison, WI), Gen Tech Rept FPL-GTR-102.
50. Cannell MGR (1982) *World Forest Biomass and Primary Production Data* (Academic, New York).
51. Enquist BJ, Niklas KJ (2002) *Science* 295:1517–1520.